How to cite: *Angew. Chem. Int. Ed.* **2021**, *60*, 24002–24007
International Edition: doi.org/10.1002/anie.202107553
German Edition: doi.org/10.1002/ange.202107553

Heterogeneous Catalysis | Hot Paper

Direct Evidence on the Mechanism of Methane Conversion under Non-oxidative Conditions over Iron-modified Silica: The Role of Propargyl Radicals Unveiled

*Allen Puente-Urbina, Zeyou Pan, Vladimir Paunović, Petr Šot, Patrick Hemberger, and Jeroen Anton van Bokhoven**

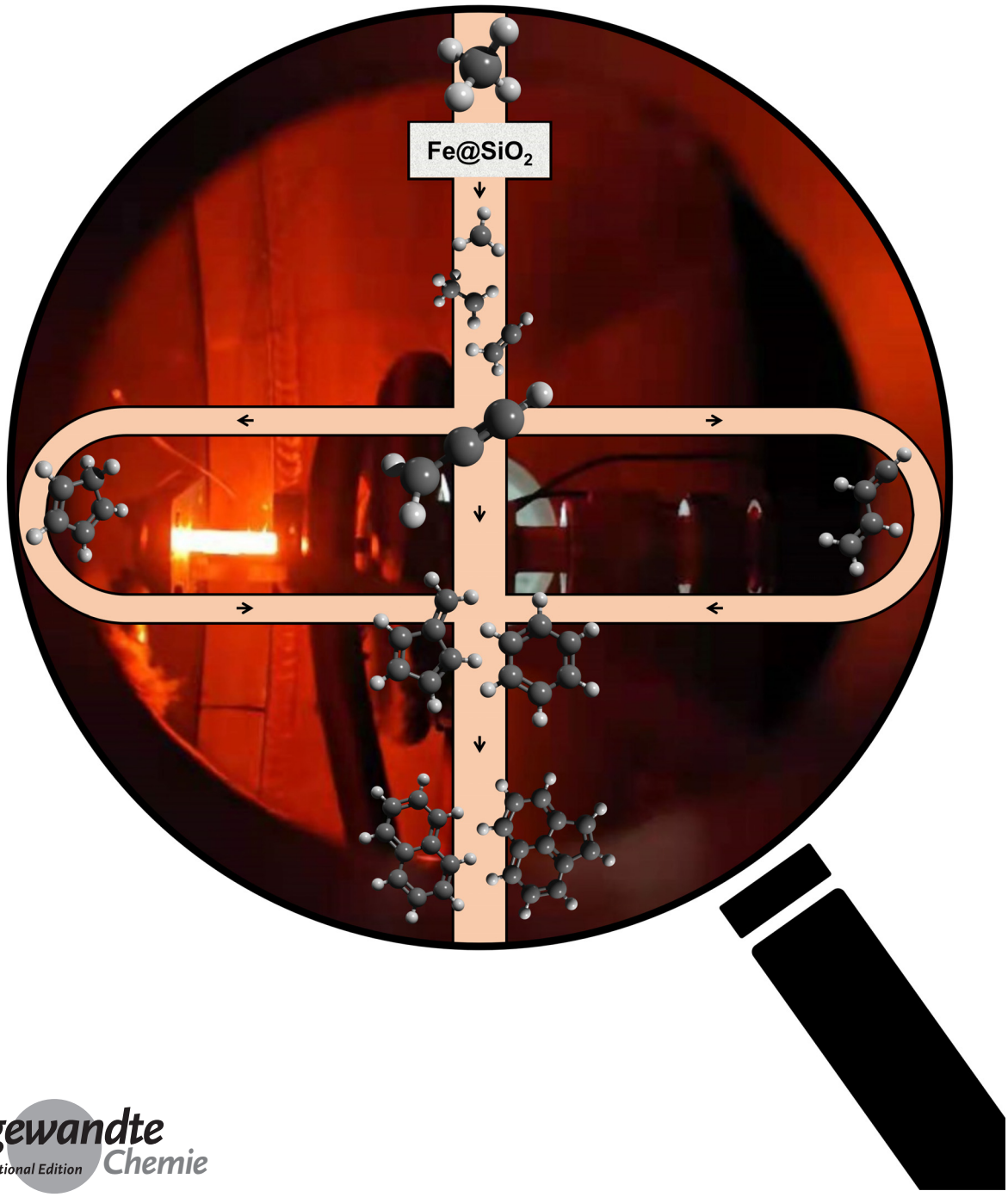

Abstract: *Radical-mediated gas-phase reactions play an important role in the conversion of methane under non-oxidative conditions into olefins and aromatics over iron-modified silica catalysts. Herein, we use operando photoelectron photoion coincidence spectroscopy to disentangle the elusive C_{2+} radical intermediates participating in the complex gas-phase reaction network. Our experiments pinpoint different C_2-C_5 radical species that allow for a stepwise growth of the hydrocarbon chains. Propargyl radicals ($H_2C{-}C{\equiv}C{-}H$) are identified as essential precursors for the formation of aromatics, which then contribute to the formation of heavier hydrocarbon products via hydrogen abstraction–acetylene addition routes (HACA mechanism). These results provide comprehensive mechanistic insights that are relevant for the development of methane valorization processes.*

Methane (CH_4) conversion under non-oxidative conditions at elevated temperatures and ambient pressure represents an attractive one-step valorization route of the abundant natural gas into C_{2+} hydrocarbons and hydrogen (H_2), which are essential platforms for the production of chemicals, polymers, and liquid fuels.[1] Different types of catalysts can be used for this process, including metal-exchanged zeolites and metal-modified oxides.[1d,2] Several recent reports pinpointed exceptional performance of iron-modified silica catalysts in this process, which displayed markedly different activity and product distribution patterns as compared to non-catalyzed methane pyrolysis under the same conditions (Table S1).[2c–m] Nonetheless, the mechanistic understanding that is essential to derive the rationale for tuning the product distribution and enhancing the catalyst lifetime is still elusive. This is mainly caused by the complexity of the process, which likely involves contributions from both surface-catalyzed and radical-mediated gas-phase pathways (Table S2).[2c–h,3] In particular, for a silica-confined single iron sites catalyst, Guo et al.[2c] proposed a reaction mechanism in which C–C bonds are formed via sequential homolytical bond dissociation reactions and stepwise chain growth. Herein, methane is activated into methyl radical ($^{\bullet}CH_3$), the coupling of which enables the formation of C_2 species (vinyl ($^{\bullet}C_2H_3$), ethyl ($^{\bullet}C_2H_5$), ethylene (C_2H_4), and ethane (C_2H_6)).[2c] Ethylene plays a key role in the next steps, as it participates in chain growth that together with dehydrogenation and cyclization reactions lead to the formation of benzene (C_6H_6) and naphthalene ($C_{10}H_8$).[2c] However, some of the elementary reaction steps, such as the formation of ethyl and vinyl radicals, lack direct experimental evidence. Furthermore, the reaction pathways and corresponding intermediates enabling the formation of C_{2+} products are still poorly understood.

Herein, we report a detailed study of the gas-phase intermediates involved in methane conversion under non-oxidative conditions using imaging photoelectron photoion coincidence (*i*PEPICO) spectroscopy (Figure S1). This technique applies tunable vacuum ultraviolet (VUV) synchrotron radiation in a collision-reduced environment to soft-ionize the gas beam entailing unconverted reactants, intermediates, and products that leave the catalytic reactor and expand into high vacuum. The ionization yields pairs of photoelectrons and photoions that are detected in delayed coincidence.[4] As a result, *i*PEPICO provides unprecedented potential to unravel complex mixtures of highly reactive gas-phase intermediates in various catalytic processes that are inaccessible by conventional analytical tools, such as gas chromatography coupled to mass spectrometry (GC-MS), due to their short lifetimes.[5]

We commence our experiments by analyzing the time-of-flight (TOF) mass spectra of the reactor effluent formed during the conversion of methane under non-oxidative conditions at ca. 945–1400 °C over iron-modified silica ($Fe@SiO_2$) catalyst (Figures 1 and 2), which has been extensively characterized in our previous study.[2i] In addition to the products that can be detected in conventional catalytic tests using reactor designs typically used to study the conversion of methane under non-oxidative conditions such as acetylene (C_2H_2, m/z 26), ethylene (C_2H_4, m/z 28), ethane (C_2H_6, m/z 30), propyne or allene (C_3H_4, m/z 40), propene (C_3H_6, m/z 42), propane (C_3H_8, m/z 44), 1,3-butadiyne (C_4H_2, m/z 50), 1-buten-3-yne (C_4H_4, m/z 52), 1,3-butadiene (C_4H_6, m/z 54), butene (C_4H_8, m/z 56), cyclopentadiene (C_5H_6, m/z 66), and fulvene or benzene (C_6H_6, m/z 78), the *i*PEPICO TOF mass spectra reveal a rich radical chemistry over iron-modified silica catalyst. Besides methyl radicals ($^{\bullet}CH_3$, m/z 15), we evidence for the first time the formation of C_{2+} radical intermediates, including vinyl ($^{\bullet}C_2H_3$, m/z 27), ethyl ($^{\bullet}C_2H_5$, m/z 29), propargyl ($^{\bullet}C_3H_3$, m/z 39), allyl ($^{\bullet}C_3H_5$, m/z 41), $^{\bullet}C_4H_3$ (m/z 51), butadienyl ($^{\bullet}C_4H_5$, m/z 53), and cyclopentadienyl ($^{\bullet}C_5H_5$, m/z 65) radicals. These short-lived intermediates are unequivocally assigned based on their m/z values, ionization energies (IE), mass-selected threshold photoelectron spectra (ms-TPES) supported by Franck-Condon (FC) simulations and photoionization (PI) spectra (Figure 1, Figures S6 and S7, and Table S4). Comparatively, the experiment performed over pure silica (SiO_2) catalyst shows only the presence of

[*] A. Puente-Urbina, Z. Pan, Dr. V. Paunović, Dr. P. Šot, Prof. Dr. J. A. van Bokhoven
Institute for Chemical and Bioengineering
Department of Chemistry and Applied Biosciences, ETH Zurich
Vladimir-Prelog-Weg 1–5/10, 8093 Zurich (Switzerland)
E-mail: jeroen.vanbokhoven@chem.ethz.ch
Z. Pan, Dr. P. Hemberger
Laboratory for Synchrotron Radiation and Femtochemistry
Paul Scherrer Institute
Forschungsstrasse 111, 5232 Villigen (Switzerland)
Dr. P. Šot
Laboratory of Inorganic Chemistry
Department of Chemistry and Applied Biosciences, ETH Zurich
Vladimir-Prelog-Weg 1–5/10, 8093 Zurich (Switzerland)
Prof. Dr. J. A. van Bokhoven
Laboratory for Catalysis and Sustainable Chemistry
Paul Scherrer Institute
Forschungsstrasse 111, 5232 Villigen (Switzerland)
Supporting information and the ORCID identification number(s) for the author(s) of this article can be found under: https://doi.org/10.1002/anie.202107553.

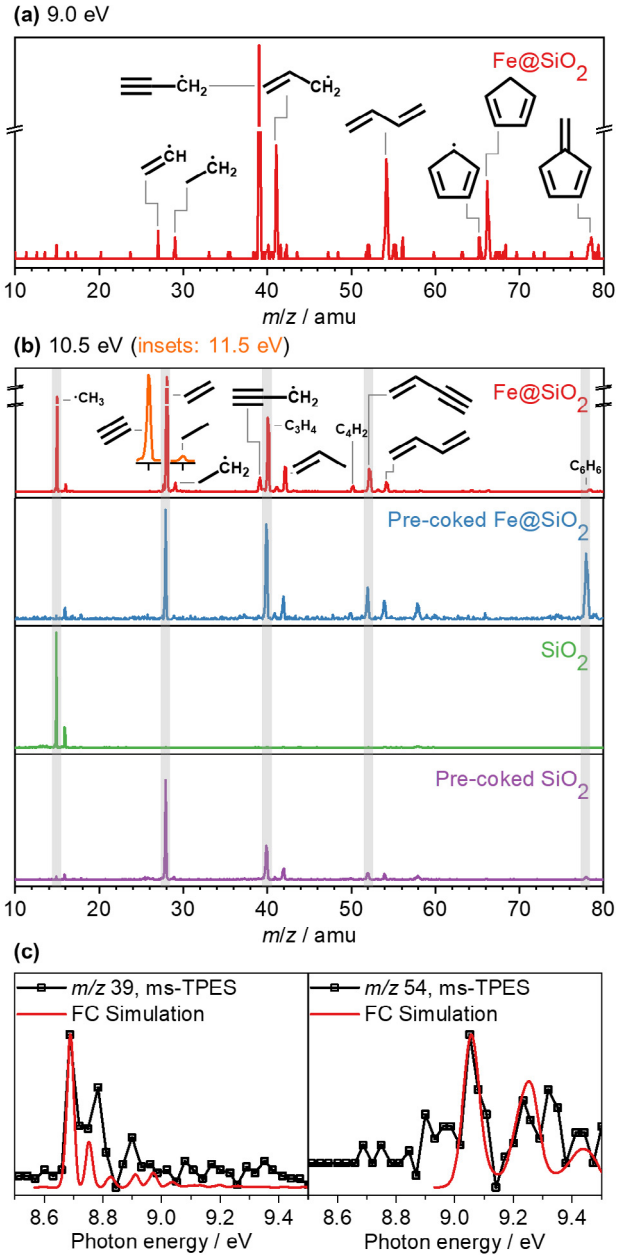

Figure 1. *i*PEPICO analysis upon conversion of methane under non-oxidative conditions over Fe@SiO_2 and SiO_2 catalysts: a),b) time-of-flight mass spectra for particular catalysts and photon energies (a: 9.0 eV; b: 10.5 eV and insets at 11.5 eV), and c) mass-selected threshold photoelectron spectra for selected *m*/*z* channels assigned isomer-specifically with the help of Franck-Condon simulations as propargyl radical (*m*/*z* 39) and 1,3-butadiene (*m*/*z* 54). Reaction conditions: F_{CH_4} = 2 sccm, c_{CH_4} = ca. 100 mol%, W_{cat} = 9.5 ± 3.8 mg, *T* = ca. 1100 °C, and *P* = 100 ± 62 mbar.

methyl radicals (Figure 1b), the concentration of which is more than one order of magnitude lower than that recorded using iron-modified silica. This result, which is consistent with a long induction period for pure silica (Figure S5),[2i] indicates that the formation of C_{2+} radicals in the early reaction stages is enabled by the iron sites. Notably, the signals of methyl, ethyl, propargyl, allyl, and cyclopentadienyl radicals together with stable products (ethylene, propyne or allene, propene, 1,3-butadiyne, 1-buten-3-yne, 1,3-butadiene, cyclopentadiene, and fulvene or benzene) are clearly visible in the TOF mass spectra acquired during methane conversion under non-oxidative conditions over pre-coked iron-modified silica (Figure 1b), implying the important role of radical intermediates during the whole course of reaction. Moreover, methyl, ethyl, and allyl are also observed along with stable hydrocarbons (ethylene, propyne or allene, propene, 1,3-butadiyne, 1-buten-3-yne, 1,3-butadiene, and fulvene or benzene) in the molecular beam stemming from the active form of pure silica catalyst, i.e., pre-coked pure silica, which also proves the participation of these radical species in the product formation.

Further insights into the role of the C_{2+} radicals are acquired by inspecting the temperature profiles (ca. 945–1400 °C) of these species in relation to the evolution of various reaction products (Figure 2 and Figure S8). At ca. 945 °C, apart from methyl, no radicals nor stable products are observed. Starting from ca. 1100 °C, the signal of methyl decreases with temperature, while ethyl presents a slight decrease in the range of ca. 1100–1230 °C and then it decreases more pronouncedly. Notably, a decrease in methyl and ethyl signals at ca. 1100–1230 °C correlates with the increase in the signals originating from vinyl, propargyl, and allyl radicals, as well as with the increase in the signals stemming from the acetylene, ethylene, ethane, propyne or allene, propene, and propane products. At higher temperature (ca. 1230–1400 °C), the intensity of methyl, vinyl, ethyl, and allyl radicals and the light products ethylene, ethane, and propene decrease, while the intensities of propargyl radical and propyne or allene increase. This is accompanied with increased production of 1-buten-3-yne, fulvene or benzene, as well as high-molecular weight and dehydrogenation products. In addition, a decrease in butadienyl and 1,3-butadiene at high temperature is coupled to the higher intensities of the 1-buten-3-yne and C_6H_6 species. Higher-molecular weight products such as *m*/*z* 102, 128, and 152, which could be phenylacetylene (C_8H_6), naphthalene ($C_{10}H_8$), and acenaphthylene ($C_{12}H_8$), constantly increase with temperature, suggesting their lower reactivity in the overall reaction scheme.

Based on this experimental evidence, the following mechanism is proposed (Figure 3 and Figure S9). Consistent with the proposal of Guo et al.,[2c] the reaction sequence starts with methane (**1**) activation by methyl radical (**2**) formation, which then couple into ethane (**3**). This initial step is facilitated by iron sites, as also corroborated by our observations on the differences in methyl radical and product concentrations between iron-modified silica and pure silica catalysts (Figure 1). Thereafter, ethane is transformed into ethyl (**4**) and ethylene (**5**) in two consecutive dehydrogenation reactions. In a similar way, ethylene is the precursor of vinyl (**6**) and acetylene (**7**). Reactions of vinyl, ethyl, and acetylene with C_1 species produce propene (**13**), propane (**12**), and allyl radical (**8**), respectively. The C_3 species propene and allyl radical can also be produced by successive dehydrogenation reactions starting from propane. Further dehydrogenations produce propyne or allene (**9**) and propargyl radical (**10**). In a side pathway, propene can also react with methyl radical and dehydrogenate to produce butene (C_4H_8, *m*/*z* 56)

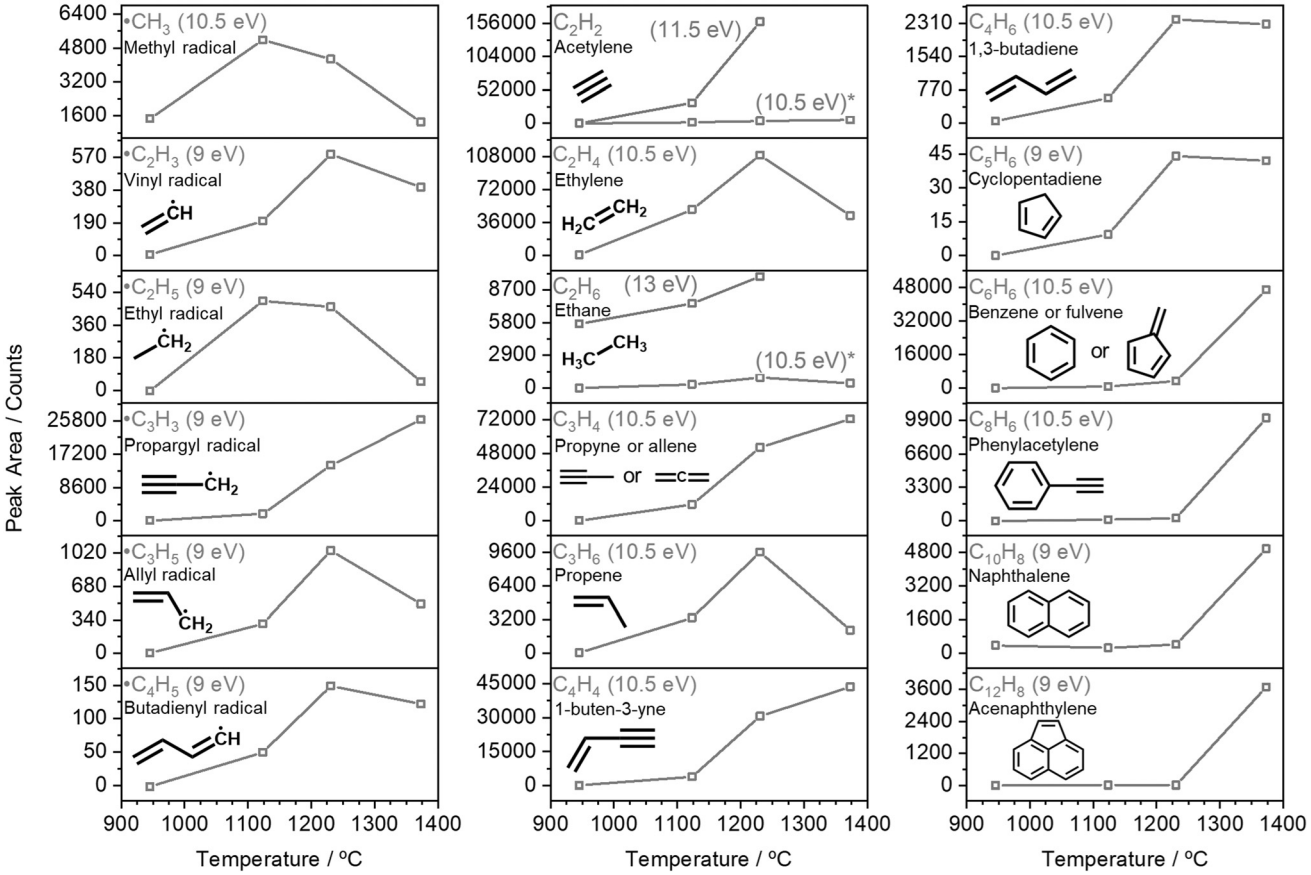

Figure 2. Evolution of radical and molecular species obtained upon conversion of methane over Fe@SiO_2 as a function of temperature analyzed by *i*PEPICO (photon energies in parentheses). Reaction conditions: F_{CH_4} = 2 sccm, c_{CH_4} = ca. 100 mol%, W_{cat} = ca. 8.0 mg, T = ca. 945–1400 °C, and P = 199.1 ± 6.8 mbar. *Species ionized with residual non-filtered high-order radiation.

and 1,3-butadiene (**16**), which can continue with dehydrogenation processes down to 1,3-butadiyne.

The propargyl radical is a key species that can react with (*i*) C_1 species to produce 1,3-butadiene, (*ii*) acetylene to produce cyclopentadienyl, or (*iii*) with another propargyl to produce the benzene (**11**) and fulvene (**15**).[6]

The tunability of the VUV photon energy in *i*PEPICO allows us to confirm the formation of both C_6H_6 isomers based on their IE (9.24 eV for benzene and 8.36 eV for fulvene).[7] The formation of C_3 species ($^{\bullet}C_3H_3$, $^{\bullet}C_3H_5$, $^{\bullet}C_3H_7$, C_3H_4, C_3H_6, and C_3H_8) as well as C_4H_6 are plausible mass growth pathways in methane conversion under non-oxidative conditions. Moreover, from 1,3-butadiene, subsequent events involving homolytic C–H bonds cleavage may produce lower-mass C_4 species down to $^{\bullet}C_4H_3$ and 1,3-butadiyne, as observed in minor concentrations.

The presence of cyclopentadienyl and cyclopentadiene is expected for high-temperature hydrocarbon reactions.[8] Cyclopentadiene (**14**) can be produced by reaction of allyl with acetylene, followed by dehydrogenation.[2j,9] Decomposition reactions of cyclopentadiene or reaction of propargyl with acetylene followed by successive dehydrogenations could lead to acyclic C_5H_4 species (*m*/*z* 64) or their respective radicals ($^{\bullet}C_5H_3$, *m*/*z* 63).[2l] These reaction pathways are corroborated by the observation of peaks at *m*/*z* values of 66, 65, 64, and 63 (Figure 4 and Figure S8).

Considering C_6H_6 species, benzene is preferred at high temperature over fulvene.[10] Benzene is not only a reaction product; it also plays an important role as a precursor for heavier species involved in the deactivation of catalysts.[11] Even though there are many proposals for benzene formation in methane conversion under non-oxidative conditions, none of them have been verified experimentally.[2j,l,6a,12] Thus, detecting benzene precursors, such as propargyl and fulvene, and understanding their production as well as consumption mechanisms is fundamental.

Miller et al.[6a] reported that propargyl can directly recombine to benzene, but also form fulvene, which then isomerizes to benzene. Our observation of both fulvene (IE = 8.36 eV) and benzene (IE = 9.24 eV) corroborates these mechanisms.[7] Scherer et al.[13] and Shafir et al.[14] pointed out that propargyl dimerizes to produce benzene or phenyl ($^{\bullet}C_6H_5$, *m*/*z* 77). Alternatively, fulvene can be formed by cyclopentadiene methylation and dehydrogenation, and may also subsequently isomerize to benzene.[12] Cyclopentadiene also decomposes to cyclopentadienyl and propargyl at high temperature, but methylation should dominate once cyclopentadienyl is formed, considering the rate constants of both processes (Table S5). Another plausible route reported by

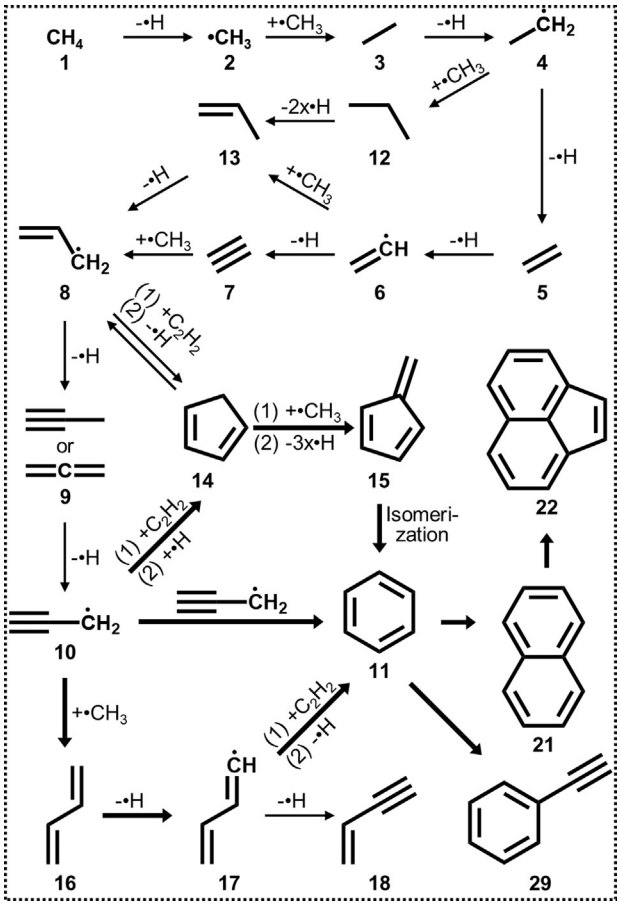

Figure 3. The mechanism of the main products formation via radical-mediated gas-phase reaction pathways in the conversion of methane under non-oxidative conditions over Fe@SiO_2 catalyst. Extended mechanism in Figure S9.

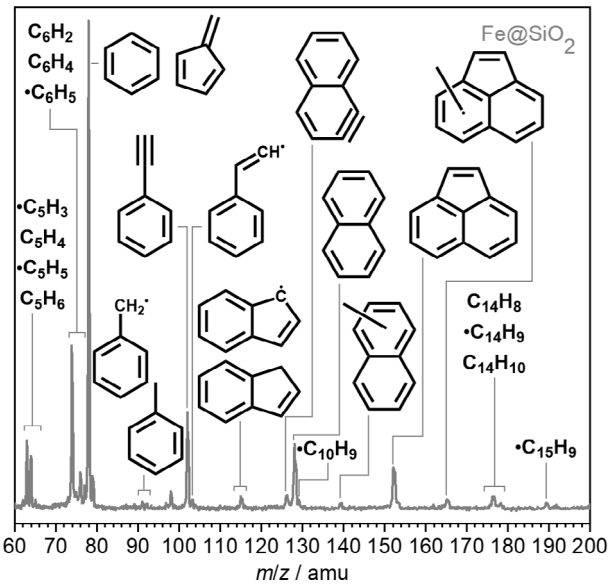

Figure 4. Time-of-flight mass spectrum obtained by *i*PEPICO using 10.5 eV of ionization energy upon conversion of methane under non-oxidative conditions over Fe@SiO_2 catalyst. Reaction conditions: F_{CH_4} = 2 sccm, c_{CH_4} = ca. 100 mol%, W_{cat} = ca. 8.0 mg, T = ca. 1400 °C, and P = ca. 204 mbar.

Dean suggests the reaction of butadienyl radical with acetylene leading to linear C_6 species, which cyclize and dehydrogenate to benzene.[2j] These routes are confirmed by our detection of the radical intermediates methyl, propargyl, butadienyl, cyclopentadienyl, and phenyl, as well as the products acetylene, cyclopentadiene, benzene and fulvene (Figures 1 and 2 and 4, and Figure S8). Even with multiple plausible pathways to produce benzene, the routes involving propargyl are the most relevant, considering the important contribution of such species evidenced experimentally (see intensity of signal at m/z 39 in Figures 1 and 2). Benzene and phenyl can provide access to other species with lower molecular weight such as C_6H_4 (m/z 76) and C_6H_2 (m/z 74) (Figure 4 and Figure S8).

High-molecular-weight species with $m/z > 78$ gain importance at higher temperature (Figures 2 and 4, and Figure S8). Their production can proceed via methylations, dehydrogenations, and the hydrogen abstraction–acetylene addition (HACA) mechanism, which are plausible at high reaction temperatures (extended description in Supporting Information).

In summary, by exploiting the unprecedented detection capabilities of the *i*PEPICO technique, it is possible to unveil elusive C_{2+} radical intermediates in methane conversion under non-oxidative conditions over iron-modified silica catalysts and to correlate their formation with the generation of different reaction products. Based on such experimental evidence, we postulate the reaction mechanisms for the formation of C_2-C_6 as well as higher molecular weight products. Resonantly stabilized propargyl radicals possess a long lifetime as shown by their large abundance and thus play a key role in the formation of the first aromatic ring, benzene. In addition, the observation of phenyl, acetylene, phenylacetylene, naphthalene, and acenaphthylene evidences the HACA reaction mechanism. Our work shows that, besides the stepwise chain growth mechanisms proposed in the literature, alternative reaction channels exist, thus provides important insights into the role of radical-mediated gas-phase reactions in conversion of methane under non-oxidative conditions over heterogeneous catalysts. The findings could help to improve the performance of this process both from a chemical and engineering point of view, as well as serve as a basis to understand other relevant catalysts such as metal-exchanged zeolites.

Acknowledgements

The authors thank the support of the VUV beamline of the Swiss Light Source located at the Paul Scherrer Institute, Villigen, Switzerland, where *i*PEPICO measurements were performed under the proposals 20191009 and 20200976. Prof. Dr. Christophe Copéret and Shell Global Solutions International B.V. are acknowledged for their collaboration and funding in previous stages of the project in which the catalysts used in this research were prepared. A.P.-U. thanks the Ministry of Science, Technology, and Telecommunications

of Costa Rica, and the Costa Rica Institute of Technology for their support. P.H. and Z.P. are grateful for the funding by Swiss National Science Foundation (SNSF, 200021_178952). P.H., Z.P., and A.P.-U. thank Patrick Ascher for technical assistance. Open access funding provided by Eidgenossische Technische Hochschule Zurich.

Conflict of Interest

The authors declare no conflict of interest.

Keywords: heterogeneous catalysis · iron · methane conversion · reaction mechanisms · silica

[1] a) L. Wang, L. Tao, M. Xie, G. Xu, J. Huang, Y. Xu, *Catal. Lett.* **1993**, *21*, 35 – 41; b) Z. R. Ismagilov, E. V. Matus, L. T. Tsikoza, *Energy Environ. Sci.* **2008**, *1*, 526 – 541; c) M. C. Alvarez-Galvan, N. Mota, M. Ojeda, S. Rojas, R. M. Navarro, J. L. G. Fierro, *Catal. Today* **2011**, *171*, 15 – 23; d) J. J. Spivey, G. Hutchings, *Chem. Soc. Rev.* **2014**, *43*, 792 – 803; e) C. Karakaya, R. J. Kee, *Prog. Energy Combust. Sci.* **2016**, *55*, 60 – 97; f) K. Huang, J. B. Miller, G. W. Huber, J. A. Dumesic, C. T. Maravelias, *Joule* **2018**, *2*, 349 – 365.

[2] a) I. Vollmer, N. Kosinov, Á. Szécsényi, G. Li, I. Yarulina, E. Abou-Hamad, A. Gurinov, S. Ould-Chikh, A. Aguilar-Tapia, J.-L. Hazemann, E. Pidko, E. Hensen, F. Kapteijn, J. Gascon, *J. Catal.* **2019**, *370*, 321 – 331; b) B. M. Weckhuysen, D. Wang, M. P. Rosynek, J. H. Lunsford, *Angew. Chem. Int. Ed. Engl.* **1997**, *36*, 2374 – 2376; *Angew. Chem.* **1997**, *109*, 2471 – 2473; c) X. Guo, G. Fang, G. Li, H. Ma, H. Fan, L. Yu, C. Ma, X. Wu, D. Deng, M. Wei, D. Tan, R. Si, S. Zhang, J. Li, L. Sun, Z. Tang, X. Pan, X. Bao, *Science* **2014**, *344*, 616; d) M. Sakbodin, Y. Wu, S. C. Oh, E. D. Wachsman, D. Liu, *Angew. Chem. Int. Ed.* **2016**, *55*, 16149 – 16152; *Angew. Chem.* **2016**, *128*, 16383 – 16386; e) S. C. Oh, E. Schulman, J. Zhang, J. Fan, Y. Pan, J. Meng, D. Liu, *Angew. Chem. Int. Ed.* **2019**, *58*, 7083 – 7086; *Angew. Chem.* **2019**, *131*, 7157 – 7160; f) S. J. Han, S. W. Lee, H. W. Kim, S. K. Kim, Y. T. Kim, *ACS Catal.* **2019**, *9*, 7984 – 7997; g) J. Hao, P. Schwach, G. Fang, X. Guo, H. Zhang, H. Shen, X. Huang, D. Eggart, X. Pan, X. Bao, *ACS Catal.* **2019**, *9*, 9045 – 9050; h) J. Hao, P. Schwach, L. Li, X. Guo, J. Weng, H. Zhang, H. Shen, G. Fang, X. Huang, X. Pan, C. Xiao, X. Yang, X. Bao, *J. Energy Chem.* **2021**, *52*, 372 – 376; i) P. Šot, M. A. Newton, D. Baabe, M. D. Walter, A. P. van Bavel, A. D. Horton, C. Copéret, J. A. van Bokhoven, *Chem. Eur. J.* **2020**, *26*, 8012 – 8016; j) A. M. Dean, *J. Phys. Chem.* **1990**, *94*, 1432 – 1439; k) O. Olsvik, F. Billaud, *Thermochim. Acta* **1994**, *232*, 155 – 169; l) D. M. Matheu, A. M. Dean, J. M. Grenda, W. H. Green, *J. Phys. Chem. A* **2003**, *107*, 8552 – 8565; m) C. Keramiotis, G. Vourliotakis, G. Skevis, M. A. Founti, C. Esarte, N. E. Sánchez, A. Millera, R. Bilbao, M. U. Alzueta, *Energy* **2012**, *43*, 103 – 110.

[3] a) P. Schwach, X. Pan, X. Bao, *Chem. Rev.* **2017**, *117*, 8497 – 8520; b) T.-H. Li, M. Yan, Y. Liu, Z.-Q. Huang, C.-R. Chang, J. Li, *J. Phys. Chem. C* **2020**, *124*, 13656 – 13663; c) Y. Liu, J.-C. Liu, T.-H. Li, Z.-H. Duan, T.-Y. Zhang, M. Yan, W.-L. Li, H. Xiao, Y.-G. Wang, C.-R. Chang, J. Li, *Angew. Chem. Int. Ed.* **2020**, *59*, 18586 – 18590; *Angew. Chem.* **2020**, *132*, 18745 – 18749; d) S. K. Kim, H. W. Kim, S. J. Han, S. W. Lee, J. Shin, Y. T. Kim, *Commun. Chem.* **2020**, *3*, 58; e) A. I. Olivos-Suarez, À. Szécsényi, E. J. M. Hensen, J. Ruiz-Martinez, E. A. Pidko, J. Gascon, *ACS Catal.* **2016**, *6*, 2965 – 2981.

[4] a) A. Bodi, B. Sztáray, T. Baer, M. Johnson, T. Gerber, *Rev. Sci. Instrum.* **2007**, *78*, 084102; b) A. Bodi, M. Johnson, T. Gerber, Z. Gengeliczki, B. Sztáray, T. Baer, *Rev. Sci. Instrum.* **2009**, *80*, 034101; c) M. Johnson, A. Bodi, L. Schulz, T. Gerber, *Nucl. Instrum. Methods Phys. Res. Sect. A* **2009**, *610*, 597 – 603.

[5] P. Hemberger, J. A. van Bokhoven, J. Pérez-Ramírez, A. Bodi, *Catal. Sci. Technol.* **2020**, *10*, 1975 – 1990.

[6] a) J. A. Miller, S. J. Klippenstein, *J. Phys. Chem. A* **2003**, *107*, 7783 – 7799; b) L. Zhao, W. Lu, M. Ahmed, M. V. Zagidullin, V. N. Azyazov, A. N. Morozov, A. M. Mebel, R. I. Kaiser, *Sci. Adv.* **2021**, *7*, eabf0360.

[7] a) F. Holzmeier, I. Fischer, B. Kiendl, A. Krueger, A. Bodi, P. Hemberger, *Phys. Chem. Chem. Phys.* **2016**, *18*, 9240 – 9247; b) G. Bieri, F. Burger, E. Heilbronner, J. P. Maier, *Helv. Chim. Acta* **1977**, *60*, 2213 – 2233.

[8] a) A. M. Scheer, C. Mukarakate, D. J. Robichaud, M. R. Nimlos, H.-H. Carstensen, G. Barney Ellison, *J. Chem. Phys.* **2012**, *136*, 044309; b) P. Hemberger, G. da Silva, A. J. Trevitt, T. Gerber, A. Bodi, *Phys. Chem. Chem. Phys.* **2015**, *17*, 30076 – 30083.

[9] J. Bouwman, A. Bodi, J. Oomens, P. Hemberger, *Phys. Chem. Chem. Phys.* **2015**, *17*, 20508 – 20514.

[10] G. Zichittella, P. Hemberger, F. Holzmeier, A. Bodi, J. Pérez-Ramírez, *J. Phys. Chem. Lett.* **2020**, *11*, 856 – 863.

[11] a) V. V. Kislov, N. I. Islamova, A. M. Kolker, S. H. Lin, A. M. Mebel, *J. Chem. Theory Comput.* **2005**, *1*, 908 – 924; b) A. M. Mebel, A. Landera, R. I. Kaiser, *J. Phys. Chem. A* **2017**, *121*, 901 – 926; c) D. S. N. Parker, R. I. Kaiser, T. P. Troy, M. Ahmed, *Angew. Chem. Int. Ed.* **2014**, *53*, 7740 – 7744; *Angew. Chem.* **2014**, *126*, 7874 – 7878.

[12] a) N. M. Marinov, W. J. Pitz, C. K. Westbrook, A. M. Vincitore, M. J. Castaldi, S. M. Senkan, C. F. Melius, *Combust. Flame* **1998**, *114*, 192 – 213; b) H. A. Gueniche, J. Biet, P. A. Glaude, R. Fournet, F. Battin-Leclerc, *Fuel* **2009**, *88*, 1388 – 1393.

[13] S. Scherer, T. Just, P. Frank, *Proc. Combust. Inst.* **2000**, *28*, 1511 – 1518.

[14] E. V. Shafir, I. R. Slagle, V. D. Knyazev, *J. Phys. Chem. A* **2003**, *107*, 8893 – 8903.

Manuscript received: June 6, 2021
Accepted manuscript online: August 29, 2021
Version of record online: September 29, 2021

